Available online at www.sciencedirect.com
ScienceDirect
Cement and Concrete Research 38 (2008) 554–564
Cement and Concrete Research

# Effect of calcium silicate sources on geopolymerisation

Christina K. Yip, Grant C. Lukey, John L. Provis, Jannie S.J. van Deventer *

*Department of Chemical and Biomolecular Engineering, University of Melbourne, Victoria 3010, Australia*

Received 28 May 2007; accepted 7 November 2007

**Abstract**

Seven different calcium silicate materials were used to investigate the role of calcium in geopolymerisation. At low alkalinity, the compressive strength of matrices prepared with predominantly amorphous calcium silicates (blast furnace slag) or containing crystalline phases specifically manufactured for reactivity (cement) is much higher than when the calcium is supplied as crystalline silicate minerals. The compressive strength of matrices containing natural (crystalline) calcium silicates improves with increasing alkalinity, however the opposite trend is observed in matrices synthesised with processed calcium silicate sources. The difference in compressive strength between matrices synthesised using different calcium silicate sources is significantly reduced at high alkalinity. An insufficient amount of calcium is dissolved from crystalline calcium silicates at relatively low alkalinity to enable formation of calcium silicate hydrate in coexistence with the aluminosilicate geopolymeric gel, and this leads to the poor mechanical properties of such matrices. At high alkalinity, calcium plays a lesser role in affecting the nature of the final binder, as it forms precipitates rather than hydrated gels. Thus, the different calcium silicate sources will not have a major impact on the mechanical properties of these matrices. The effects of different calcium silicates on geopolymerisation are therefore seen to depend most significantly on two factors: the crystallinity of the calcium silicate source, and the alkalinity of the activating solution used.


*Keywords:* Geopolymer; Microstructure; Characterisation; Mechanical properties; Metakaolin

## 1. Introduction

Geopolymers have been shown to offer an environmentally friendly, technically competitive alternative to ordinary Portland cement (OPC) [1–5], and are beginning to be more widely utilised in various applications. However, many mechanistic aspects of geopolymerisation are not yet well understood. Previous studies have shown that the addition of calcium has a generally positive effect on the mechanical properties of the geopolymeric binder [6–11], but the exact role of calcium during the geopolymerisation process remains unclear. Phase separation between alkali-aluminosilicate (i.e. geopolymer) and partially Al-substituted calcium silicate hydrate (C-A-S-H) gels has been observed in a number of Ca-containing geopolymer systems [8,9,12–17].

It has also been suggested, but never definitively proven, that $Ca^{2+}$ is capable of acting as a charge-balancing cation within the geopolymeric binder structure [1]. If this is the case, then there may also be significant implications with respect to Si/Al ordering within the geopolymeric network structure, as $Ca^{2+}$ is known to greatly reduce the energy penalty associated with Si/Al ordering violation in aluminosilicate networks in aluminosilicate glasses [18]. Si/Al ordering in geopolymers will be important in key applications such as waste immobilisation [19], and ordering violations induced by the presence of $Ca^{2+}$ in charge-balancing sites may therefore be of significant practical interest.

The gel phase in geopolymer cements reinforced with wollastonite ($CaSiO_3$) fibres has been observed to bind to the fibre surfaces [20], indicating that there is some chemical interaction occurring in this system between the gel and the mineral, even with calcium silicate present in highly crystalline form. Studies of adhesion of geopolymers to natural siliceous rock surfaces [21,22] show that chemical interactions between the binder and

* Corresponding author. Tel.: +61 3 8344 9737; fax: +61 3 8344 7707.
*E-mail address:* jannie@unimelb.edu.au (J.S.J. van Deventer).

0008-8846/$ - see front matter © 2007 Elsevier Ltd. All rights reserved.
doi:10.1016/j.cemconres.2007.11.001

the rock are highly significant in determining both the bond strength and also the physicochemical properties of the geopolymeric binder in the region immediately adjoining the rock surface. These same rocks are often considered 'inert' aggregates in OPC systems (although the exact nature of this role is still under discussion), suggesting that the role of particulate inclusions in the geopolymer structure is much more of an active one than is observed in OPC, and suggesting that the differences between calcium-containing minerals with varying silicate network structures may be significant in the context of their addition to geopolymers.

In the current study, seven different calcium silicate materials, natural and processed, are added to a geopolymeric binder synthesised by the alkaline activation of metakaolin. This paper will focus on the interrelationship between the dissolution rate of the different species in the original calcium silicate materials and the mechanical properties and nature of the resultant geopolymer products. The findings of this study are fundamental to further work investigating the role of calcium in geopolymerisation.

## 2. Experimental procedures

### 2.1. Materials

Seven different calcium silicate sources were used in this study, as listed in Table 1. Ground granulated blast furnace slag (GGBFS) was obtained from Independent Cement, Australia, with a $d_{50}$ of 15.14 μm and $d_{10}$ of 2.5 μm. Cement was obtained from Geelong Cement Limited, Australia, with a $d_{50}$ of 28.13 μm, $d_{10}$ of 8.2 μm, and 100% passing a 63 μm sieve. Wollastonite ($CaSiO_3$) was purchased from Claywork, Australia. All other minerals were purchased from Geological Specimen Supplies, Australia, and had a particle size distribution of $d_{50} \sim 15$–30 μm, with 100% passing a 63 μm sieve. Laboratory grade (98% purity) $Ca(OH)_2$ manufactured by Ajax Chemicals was also used as a source of calcium.

Metakaolin was used as the primary aluminosilicate source for geopolymerisation, and was obtained from ECC International under the brand name of MetaStar 402 with a particle size distribution of 100% <20 μm and a $d_{50}$ of 1.6 μm. The oxide compositions of all materials used are presented in Table 1; these were obtained by X-Ray Fluorescence (XRF) analysis using a Siemens SRS 3000 instrument.

The commercial metakaolin used contains a minor crystalline impurity identified as muscovite-3T, Powder Diffraction File (PDF) #07-0042. The wollastonite sample used has a very small amount of a phase tentatively identified as aerinite (PDF #46-1369), and the hornblende contains some augite (PDF #24-0201). The tremolite sample contains some calcite as well as a small amount of magnesioriebeckite (PDF #20-0656), and the anorthite also shows some cordierite (PDF #13-0294) as well as a very small amount of one or more forms of the crystal forms of illite (exact symmetry not able to be determined due to the small quantity present). The prehnite sample used does not show any notable crystalline impurities. Each of these impurities identified is estimated to comprise less than 5–10% of the total mineral content.

The sodium silicate solution used in each experiment was supplied by PQ Australia, under the brand name Vitrosol N48 with 28.7% $SiO_2$, 8.9% $Na_2O$ and 62.4% $H_2O$; density 1370 kg/m$^3$. Sodium hydroxide pearl (99% purity) was purchased from Orica Australia. Distilled water was used throughout the work. Fine washed quartz sand (100% <2 mm, Commercial Minerals, Australia) was used as the aggregate to make mortar samples for compressive strength testing.

### 2.2. Synthesis

Standard (control) calcium-free geopolymeric binders (Matrices S1, S2 and S3) were prepared by mixing metakaolin with three different sets of sodium silicate activating solutions prepared from commercial sodium silicate solutions and NaOH pearl at molar ratios $R = SiO_2/Na_2O = 2.0$, 1.5 and 1.2. All solutions had the same dissolved silica content, with $R$ adjusted by the addition of NaOH to the commercial sodium silicate solution. The mass ratio between metakaolin and the alkaline activator was 0.69 for $R = 2.0$, 0.65 for $R = 1.5$, and 0.61 for $R = 1.2$. These ratios correspond to water/binder ratios of 0.442, 0.416 and 0.390 respectively.

For each calcium silicate material CS, matrices were synthesised using a MK/(MK + CS) mass ratio of 0.8 and 0.6 using each of the three activating solutions. MK and CS were mixed thoroughly, and the activator solution was then stirred with the dry mix to form a paste which was then mixed for a further 3 min. To synthesise mortar samples for compressive strength testing, washed sand was gradually added to the homogeneous paste until a uniform mixture was formed with a mass ratio of

Table 1
Chemical analysis of source materials (mass %, from XRF)

| Material | Abbreviation | CaO | $SiO_2$ | $Al_2O_3$ | $Fe_2O_3$ | MgO | $K_2O$ | $Na_2O$ |
|---|---|---|---|---|---|---|---|---|
| Metakaolin | MK | 0.10 | 54.8 | 40.42 | 0.76 | 0.41 | 2.72 | 0.07 |
| Slag [a] | GGBFS | 43.0 | 34.4 | 14.1 | 0.11 | 6.3 | 0.33 | 0.3 |
| Cement | CEM | 64.7 | 20.45 | 4.58 | 3.72 | 1.67 | 0.39 | 0.67 |
| Wollastonite | WOL | 47.5 | 50.5 | 0.25 | 0.2 | 0.25 | 0.33 | 0.3 |
| Hornblende | HRN | 21.39 | 50.4 | 0.95 | 11.96 | 11.52 | 0.04 | 1.83 |
| Tremolite | TRM | 22.57 | 44.53 | 1.68 | 2.03 | 18.74 | 0.09 | 0.17 |
| Prehnite | PRH | 25.77 | 42.23 | 22.73 | 1.72 | 0.1 | 0.01 | 0.09 |
| Anorthite | ANO | 15.43 | 47.38 | 31.02 | 0.84 | 1.42 | 0.57 | 1.26 |

[a] Ground granulated blast furnace slag, containing gypsum additive.

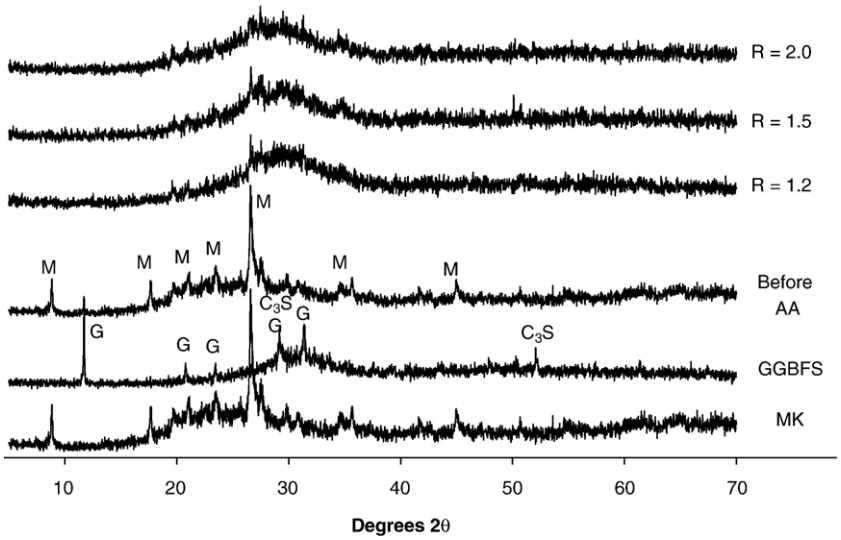


Fig. 1. X-ray diffractograms of metakaolin, GGBFS, dry mixed sample (20% GGBFS and 80% MK) before alkali activation, and geopolymer binders at 28 days (Matrices A1, A3 and A5) synthesised using $R=2.0$, 1.5 and 1.2. M: muscovite, G: gypsum, $C_3S$: tricalcium silicate.

sand/(MK+CS)=3. The geopolymer slurry was then poured into moulds and cured in a laboratory oven at 40 °C for 24 h, demoulded and aged at 25 °C prior to strength testing at 7 and 28 days.

### 2.3. Analytical techniques

To determine the leachability of Ca, Si and Al from the raw materials used, suspensions were prepared with the minerals leaching in 2.5, 5 and 7.5 M NaOH. Each suspension contained 50 g of solid in 100 mL of NaOH solution. Samples of the suspensions during mixing were taken at 1 h and 24 h centrifuged, filtered (0.2 μm Minisart membrane filter, Sartorius AG, Germany) and diluted with 10% HCl for analysis by inductively coupled plasma-optical emission spectroscopy (ICP-OES) (Perkin-Elmer 3000).

Compressive strength testing was performed as per Australian Standard (AS1012.9-1999), using the average of three 50 mm diameter cylinders with an aspect ratio of 2.0. While the Standard is specified for testing of concretes, the procedure was also found to give good results for the mortar specimens used here and so was applied unmodified. All samples were tested at 7 and 28 days using an ELE International Auto Test Compression Machine. The top face of the specimen was cut parallel to the bottom face with a diamond saw prior to testing. The top surface of the sample was capped with fast setting Boral Dental Plaster where necessary to ensure the correct aspect ratio.

X-ray diffractograms were recorded on a PHILIPS PW1800 machine using Cu $K_\alpha$ radiation and a scanning rate of 2°/min from 5 to 70° $2\theta$. The specimens were prepared by mechanical grinding using a ring mill.

## 3. Results and discussion

### 3.1. Characterisation of calcium silicate materials

Two processed materials (GGBFS and cement) and five natural calcium silicate minerals were used in this study. These

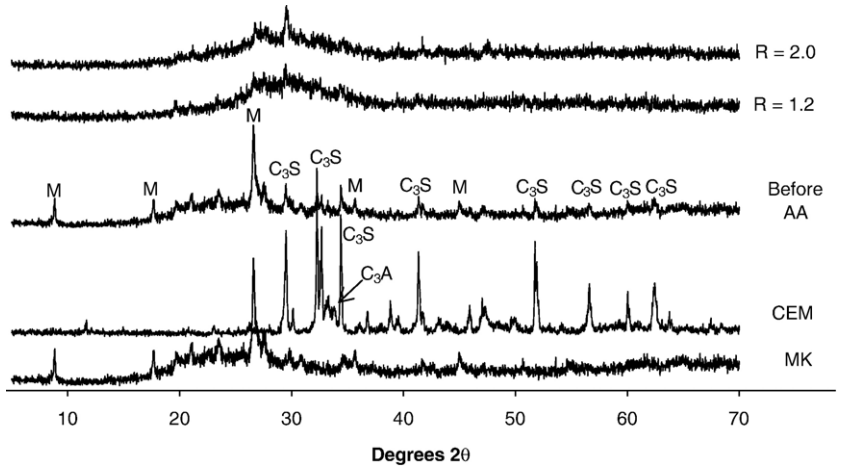


Fig. 2. X-ray diffractograms of metakaolin, cement, dry mixed sample (20% CEM and 80% MK) before alkali activation, and geopolymer binders at 28 days (Matrices B1 and B5) synthesised at $R=2.0$ and 1.2. M: muscovite, $C_3S$: tricalcium silicate, $C_3A$: tricalcium aluminate.

Table 2
Physical properties of source materials

| Material | Crystallinity | Group | Ideal toichiometry | Hardness (Mohs) | Density (g/cm$^3$) |
|---|---|---|---|---|---|
| GGBFS | Amorphous | – | – | – | |
| CEM | Largely crystalline | – | – | – | – |
| WOL | Crystalline | Inosilicate | $CaSiO_3$ | 4.8 | 2.9 |
| HRN | Crystalline | Inosilicate | $Ca_2(Mg,Fe,Al)_5(Al,Si)_8O_{22}(OH)_2$ | 5.5 | 3.2 |
| TRM | Crystalline | Inosilicate | $Ca_2Mg_5Si_8O_{22}(OH)_2$ | 5.5 | 3.0 |
| PRH | Crystalline | Phyllosilicate | $Ca_2Al_2Si_3O_{10}(OH)_2$ | 2.9 | 6.3 |
| ANO | Crystalline | Tectosilicate | $CaAlSi_3O_8$ | 6.3 | 2.8 |

seven materials cover a range of elemental compositions, mineralogy, crystal structure, and thermal history (Table 1).

It is well known that GGBFS is essentially an amorphous calcium silicate material. However, it is common practice in Australia to blend gypsum with slags during grinding. As a result, it is shown by XRD (Fig. 1) that gypsum (PDF # 33-0311) is the major crystalline phase present in the GGBFS used in this study, along with small amounts of tricalcium silicate (PDF #42-0551). Cement contains several crystalline and semi-crystalline phases, in particular tricalcium silicate and tricalcium aluminate (Fig. 2).

As indicated in Table 2, the five natural silicate minerals used in the study cover a number of crystal structures in the silicate class of minerals. Wollastonite, hornblende and tremolite are all inosilicates, with wollastonite belonging to the single chain group and hornblende and tremolite belonging to the double chain group. Prehnite is a phyllosilicate and thus contains silicate sheets. The sheets of prehnite are typically interconnected via layers of cations, which are weakly bonded and often have water or other molecules trapped (intercalated) between the sheets. Correspondingly, prehnite has a much lower hardness than the other silicate minerals (Table 2). Anorthite (calcium plagioclase) is a framework silicate (tectosilicate) belonging to the feldspar group. Aluminium can substitute for up to 50% of the silicon in the tetrahedral network structure in tectosilicates, and is charge-balanced by extraframework cations, calcium in the case of anorthite here.

### 3.2. Reactivity of calcium silicates

The dissolution of silicon and aluminium from the aluminosilicate source (metakaolin in this case) governs the initial stage of geopolymerisation [5,6,23,24]. The formation of a geopolymeric gel depends on the availability of dissociated silicate $SiO_n(OH)_{4-n}^{n-}$ and aluminate $Al(OH)_4^-$ monomers in the alkaline medium, which is further dependent on the extent of dissolution of these two species from the original aluminosilicate source. In the presence of soluble calcium species, the governing reactions may become more complex. Under these circumstances, calcium could either (1) precipitate as $Ca(OH)_2$, lowering the alkalinity of the medium and thus the driving force for dissolution of silicon and aluminium, or (2) interfere with the formation of the geopolymeric gel by reacting with the dissolved silicate and aluminate species. Thus, the interaction between calcium, silicon and aluminium species in an alkaline medium is expected to have a highly significant impact on the nature of the resultant product.

Tables 3 and 4 present the concentrations of Si, Al and Ca in solution after 1 h and 24 h of contact between each calcium silicate material and NaOH solutions of different concentrations,

Table 3
Concentration (ppm) of Ca, Si and Al from calcium silicate materials dissolved in NaOH solutions after 1 h leaching, as well as percentage of total element inventory that has been leached (in italics)

| Material | 2 M NaOH | | | 5 M NaOH | | | 7.5 M NaOH | | |
|---|---|---|---|---|---|---|---|---|---|
| | Ca | Si | Al | Ca | Si | Al | Ca | Si | Al |
| GGBFS | 53 | 379 | 159 | 764 | 2390 | 329 | 256 | 1275 | 286 |
| | *0.03%* | *0.47%* | *0.43%* | *0.41%* | *2.97%* | *0.88%* | *0.14%* | *1.59%* | *0.77%* |
| CEM | 96 | 89 | 3 | 155 | 1602 | 13 | 461 | 1535 | 35 |
| | *0.03%* | *0.19%* | *0.02%* | *0.06%* | *3.35%* | *0.11%* | *0.16%* | *3.21%* | *0.29%* |
| WOL | 46 | 41 | 1 | 206 | 113 | 4 | 239 | 31 | 3 |
| | *0.02%* | *0.03%* | *0.15%* | *0.10%* | *0.10%* | *0.60%* | *0.12%* | *0.03%* | *0.45%* |
| HRN | 125 | 84 | 9 | 281 | 117 | 39 | 61 | 127 | 49 |
| | *0.13%* | *0.07%* | *0.36%* | *0.30%* | *0.10%* | *1.55%* | *0.07%* | *0.11%* | *1.95%* |
| TRM | 96 | 89 | 5 | 875 | 106 | 19 | 63 | 82 | 14 |
| | *0.10%* | *0.09%* | *0.11%* | *0.89%* | *0.10%* | *0.43%* | *0.06%* | *0.08%* | *0.31%* |
| PRH | 73 | 511 | 382 | 125 | 638 | 515 | 168 | 482 | 543 |
| | *0.07%* | *0.52%* | *0.64%* | *0.11%* | *0.65%* | *0.86%* | *0.15%* | *0.49%* | *0.90%* |
| ANO | 43 | 486 | 353 | 436 | 607 | 232 | 138 | 681 | 713 |
| | *0.06%* | *0.44%* | *0.43%* | *0.65%* | *0.55%* | *0.28%* | *0.21%* | *0.61%* | *0.87%* |

Table 4
Concentration (ppm) of Ca, Si and Al from calcium silicate materials dissolved in NaOH solutions after 24 h leaching, as well as percentage of total element inventory that has been leached (in italics)

| Material | 2 M NaOH | | | 5 M NaOH | | | 7.5 M NaOH | | |
|---|---|---|---|---|---|---|---|---|---|
| | Ca | Si | Al | Ca | Si | Al | Ca | Si | Al |
| GGBFS | 16 | 228 | 210 | 195 | 1213 | 1035 | 75 | 1990 | 665 |
| | *0.01%* | *0.28%* | *0.56%* | *0.10%* | *1.51%* | *2.77%* | *0.04%* | *2.48%* | *1.78%* |
| CEM | 58 | 82 | 8 | 336 | 440 | 28 | 285 | 669 | 57 |
| | *0.02%* | *0.17%* | *0.07%* | *0.12%* | *0.92%* | *0.23%* | *0.10%* | *1.40%* | *0.47%* |
| WOL | 28 | 125 | 21 | 799 | 536 | 71 | 1090 | 284 | 16 |
| | *0.01%* | *0.11%* | *3.17%* | *0.39%* | *0.45%* | *10.73%* | *0.53%* | *0.24%* | *2.42%* |
| HRN | 303 | 143 | 21 | 392 | 456 | 35 | 196 | 911 | 71 |
| | *0.33%* | *0.12%* | *0.84%* | *0.42%* | *0.39%* | *1.39%* | *0.21%* | *0.77%* | *2.82%* |
| TRM | 250 | 144 | 8 | 244 | 483 | 6.0 | 612 | 511 | 25 |
| | *0.25%* | *0.14%* | *0.18%* | *0.25%* | *0.46%* | *0.13%* | *0.62%* | *0.49%* | *0.56%* |
| PRH | 342 | 863 | 1390 | 265 | 1142 | 1361 | 134 | 1888 | 1119 |
| | *0.31%* | *0.87%* | *2.31%* | *0.24%* | *1.16%* | *2.26%* | *0.12%* | *1.91%* | *1.86%* |
| ANO | 92 | 927 | 1625 | 181 | 1139 | 1475 | 66 | 2370 | 1949 |
| | *0.14%* | *0.84%* | *1.98%* | *0.27%* | *1.03%* | *1.80%* | *0.10%* | *2.14%* | *2.37%* |

as well as the total percentage of each element that has been leached. GGBFS and cement both show a relatively rapid rate of leaching in 5 M NaOH and in 7.5 M NaOH, consistent with their lower crystallinity. However, in both 2 M and 5 M NaOH but less significantly at 7.5 M, the concentrations of the leached species are lower at 24 h than at 1 h, indicating that a reprecipitation reaction has taken place. This is consistent with the tendency of both of these materials to form hydrated cementitious phases upon contact with water, which appears to be impeded slightly, but not completely, by very high alkalinity.

Anorthite (framework structure) and prehnite (sheet structure) consistently show a much higher extent of dissolution than any other minerals tested. This is quite possibly due significantly to the very much higher Al content of these minerals compared to the inosilicates tested here. Oelkers et al. [25] noted that feldspars (such as anorthite) will dissolve by a process involving first removal of non-framework cations, then selective leaching of Al via breakage of the weakened Al–O–Si linkages, then leaching of silica from the remnant, significantly disrupted and depolymerised network. Faster dissolution of more highly coordinated silicate minerals may seem somewhat counterintuitive, as more bond breakages are required to release each Si or Al atom from the mineral structure. However, the disruption caused by removal of Al from these structures is underlying the observed behaviour. Xu and van Deventer [23] did not observe a strong correlation between Al content and cation (Si, Al) leachability in hydroxide solutions. However, analysis of their data in this context will be significantly complicated by the fact that many of the minerals selected for analysis in that study contained Al predominantly in coordinations other than Al(IV), meaning that the depolymerisation and network-disruption mechanisms that cause high leachability of Si from feldspars will not be specifically applicable.

Amongst the three inosilicates used in the current study, the single chain wollastonite has a consistently lower extent of dissolution than the two double chain silicates, hornblende and tremolite. This appears to conflict with the observations of Brantley and Chen [26] and of Golubev et al. [27], who found that wollastonite consistently dissolved more rapidly than hornblende, under either alkaline or acidic conditions. However, under the conditions employed in the batch leaching experiments, it is entirely possible that precipitation of calcium silicate hydrate phases from the high concentrations of available Ca and Si species in the wollastonite leaching system has reduced the apparent leach rate to below that of the less active hornblende and tremolite. Consistent with this suggestion is the observation that the Ca release from wollastonite in the highest-alkalinity leaching system is much higher than from hornblende or tremolite, corresponding to the reduced tendency towards C-S-H formation at very high pH.

Tables 3 and 4 do not show a clear relationship between the mineralogy of calcium silicate sources and the extent of dissolution of calcium. Also, there is no clear correlation between the concentration of calcium and the concentrations of silicon and aluminium at any given condition. The primary trend that can be noted is that the extent of leaching into 5 M NaOH is in general greater than in either 2 M or 7.5 M NaOH. This cannot be explained by simple ionic activity or pH considerations, but rather suggests that there is competition between the increased pH in more concentrated NaOH solutions and the increased tendency for hydroxide species (particularly $Ca(OH)_2$ and to a lesser extent $Al(OH)_3$) to precipitate in the presence of higher concentrations of $OH^-$. In the absence of significant levels of dissolved calcium, silicate and aluminate monomers will react together to form a geopolymer in an alkaline environment. Any calcium hydroxide precipitation will lower the alkalinity of the solution and therefore the driving force for mineral dissolution, potentially hindering the formation of geopolymer gel.

However, it has also been observed that addition of calcium in any of a number of soluble or sparingly soluble forms, even at relatively low levels, will significantly accelerate the setting and hardening of geopolymerisation slurries [28]. It may be that the precipitation of $Ca(OH)_2$ or calcium silicate hydrates from the solution provides nucleation sites which then trigger rapid

Table 5
Compressive strengths (MPa) of matrices synthesised at different $R$ ratios

| Calcium silicate material (CS) | MK/MK+CS | Matrix | $R$=2.0 | | Matrix | $R$=1.5 | | Matrix | $R$=1.2 | |
|---|---|---|---|---|---|---|---|---|---|---|
| | | | 7-day (MPa) | 28-day (MPa) | | 7-day (MPa) | 28-day (MPa) | | 7-day (MPa) | 28-day (MPa) |
| None | 1 | S1 | 34.6 | 35.2 | S2 | 62.0 | 65.0 | S3 | 36.2 | 38.4 |
| GGBFS | 0.8 | A1 | 47.1 | 54.2 | A3 | 45.3 | 46.8 | A5 | 38.6 | 40.5 |
| | 0.6 | A2 | 41.5 | 52.7 | A4 | 38.6 | 39.3 | A6 | 25.4 | 26.0 |
| CEM | 0.8 | B1 | 47.5 | 53.5 | B3 | 49.3 | 56.8 | B5 | 46.2 | 51.4 |
| | 0.6 | B2 | 31.2 | 28.1 | B4 | 35.4 | 35.1 | B6 | 32.2 | 33.8 |
| WOL | 0.8 | C1 | <5.0 | 18.8 | C3 | 36.5 | 38.2 | C5 | 22.7 | 25.3 |
| | 0.6 | C2 | <5.0 | 16.8 | C4 | 19.3 | 24.3 | C6 | 14.0 | 20.8 |
| HRN | 0.8 | E1 | <5.0 | 8.3 | E3 | 31.1 | 36.7 | E5 | 32.3 | 37.0 |
| | 0.6 | E2 | <5.0 | 5.7 | E4 | 21.3 | 23.3 | E6 | 17.3 | 22.4 |
| TRM | 0.8 | G1 | N/A | N/A | G3 | 31.7 | 38.3 | G5 | 27.8 | 35.3 |
| | 0.6 | G2 | N/A | N/A | G4 | 26.5 | 28.6 | G6 | 19.5 | 25.4 |
| PRH | 0.8 | F1 | 6.7 | 14.3 | F3 | 32.2 | 39.4 | F5 | 29.5 | 36.4 |
| | 0.6 | F2 | 6.2 | 11.5 | F4 | 24.0 | 25.1 | F6 | 14.0 | 21.2 |
| ANO | 0.8 | D1 | N/A | N/A | D3 | 29.3 | 35.3 | D5 | 26.2 | 28.7 |
| | 0.6 | D2 | N/A | N/A | D4 | 18.8 | 22.1 | D6 | 15.8 | 20.3 |

Samples marked N/A were insufficiently set to be demoulded after 24 h.

geopolymer gel formation. Further work in this area is ongoing, but this hypothesis does appear to hold some merit.

### 3.3. Effects on compressive strength

The compressive strengths of the matrices synthesised using different calcium silicate materials and different alkali silicate activators are summarised in Table 5. The compressive strengths of matrices prepared with ANO and TRM at $R$=2.0 are not shown because these matrices failed to set sufficiently for demoulding.

Several key trends are observed in Table 5:

- The strengths of the samples with $R$=1.5 are higher than those with either $R$=1.2 or 2.0, both with and without the addition of calcium silicate minerals, consistent with the data of Duxson et al. for Ca-free systems [29,30]. However, the difference between $R$=1.5 and 1.2 is reduced by the addition of calcium silicate minerals.
- The compressive strengths of the binders synthesised with moderate additions of cement and GGBFS were higher than all other binders synthesised using natural calcium silicate minerals.
- 20% substitution of any calcium silicate material provides higher strength than 40%. 40% calcium silicate addition causes a significant decrease in strength compared to the control samples in almost all cases, even in the cases where 20% is beneficial.
- Addition of any crystalline calcium silicate mineral to geopolymers with $R$=2.0 results in a dramatically decreased strength, whereas both slag and cement provide an increase in strength at this relatively low alkalinity (pH ~ 11–12).
- Addition of any calcium silicate source to geopolymers with $R$=1.5 leads to a decrease in strength. This decrease is smaller for slag and cement than for any of the natural calcium silicates.
- Addition of 20% slag or cement to geopolymers with $R$=1.2 is beneficial for strength, but 40% is detrimental. Addition of any natural calcium silicate mineral gives a decrease in strength, however the effect is generally small at 20% addition.
- In almost all cases, the 7-day strength is very close to the value attained after 28 days.
- The effect of varying NaOH concentration on the geopolymers containing cement is much less than in any other systems.

It must be noted that the calcium silicate minerals show a significantly larger particle size than the metakaolin, which may become significant in analysis of their respective reactivities. Nonetheless, explanations for some of these trends may be provided based on analysis of the leaching data and other existing knowledge regarding the chemistry of geopolymerisation.

The observation that an optimum in strength occurs at $R$=1.5 is related to the microstructure of the geopolymeric binder and has been analysed previously [29,30]. This will therefore not be discussed in detail here other than to note that the addition of calcium silicate materials appears not to have significantly altered the trends in geopolymer gel microstructure observed in Ca-free systems, as would be expected if $Ca^{2+}$ is not playing a significant charge-balancing role within the geopolymer gel network structure.

It does appear that the presence of even a small amount of $Ca^{2+}$ is sufficient to disrupt the optimal geopolymer gel binder structure sufficiently to hinder strength development. However, this may also be attributed to local alteration of the binder Si/Al ratio near the calcium silicate particles by leaching of Si and/or Al, providing regions of less-than-optimal microstructure which act as flaws in the matrix under compressive strength testing.

The dramatic reduction in strength upon addition of crystalline calcium silicates to metakaolin-based geopolymers with $R$=2.0 is attributed to the low reactivity of these silicate materials during geopolymerisation. The 1 h leaching data are probably most representative of the timescales on which the geopolymer slurry is sufficiently fluid for significant leaching of the calcium silicate minerals to occur. Leaching in 2 M NaOH

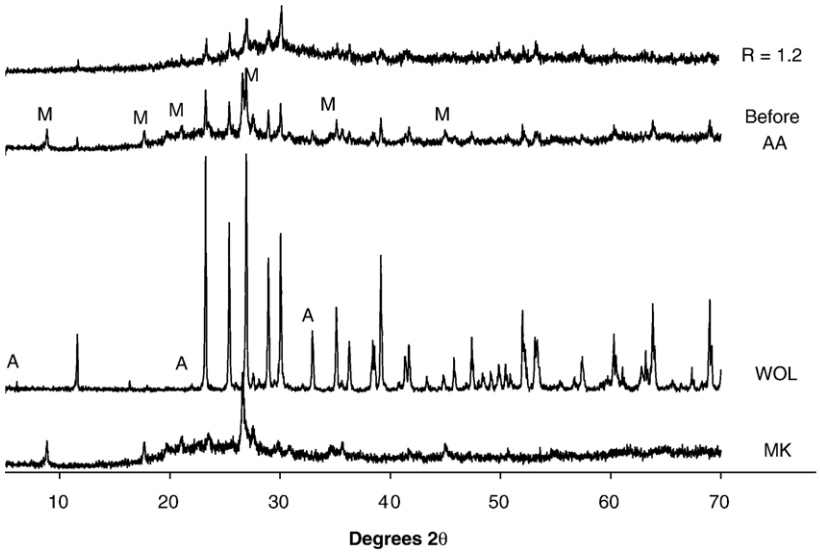


Fig. 3. XRD patterns of metakaolin, wollastonite, dry mixed sample (20% WOL and 80% MK) before alkali activation, and geopolymer binder at 28 days (Matrix C5) synthesised at $R=1.2$. M: muscovite, A: aerinite, all unlabelled major peaks are due to wollastonite.

provides a significantly more alkaline environment than is present in a silicate solution at $R=2.0$, and even so the extent of dissolution of the natural minerals in 1 h under these conditions (Table 3) is low. The alkalinity of the activating solution is not sufficient even to etch the particle surfaces to the extent where they may be considered bound to the gel by surface interactions after 7 days. So, the primary role of the added minerals is to disrupt the geopolymer gel network, leading to a very low-strength product. Similar effects have been noted in the addition of $ZrO_2$ particles to fly ash geopolymers, where any more than 3% $ZrO_2$ caused a decrease in geopolymer strength by a similar network-disruption effect [31].

After 28 days of ageing, some of the mineral surfaces (most notably wollastonite) will have been etched somewhat by the alkaline conditions, and so have begun to interact with the geopolymer gel, giving a significant increase in strength compared to 7 days. Addition of more NaOH to the activating solutions ($R=1.5$ or 1.2) enhances these interactions further, reducing the network-disrupting effects of the relatively unreactive mineral phases and increasing strength. The fact that the strength and leachability trends do not exactly correlate suggests that there is a surface-controlled mechanism of incorporation of the unreacted particles into the geopolymer gel network. The relative strengths of the surface binding of geopolymer gel to the different mineral phases will not necessarily follow a trend exactly matching their leachability. Also, particle shape and mechanical interlocking effects may also be significant, meaning that macroscopic compressive strength may not be a reliable measure of the microscopic surface binding. Analysis such as that conducted by Lee and van Deventer [21,22] for siltstone aggregate particles is therefore necessary to determine these effects exactly.

At $R=2.0$, the metakaolin is not able to release sufficient aluminate and silicate species to promote the formation of a strong geopolymer microstructure [29], and thus the compressive strength of the resultant binder is lower. However, 20% cement or GGBFS is observed from Table 3 to improve strength. The alkaline activation of GGBFS and cement will lead to the formation of some new phases that may assist the geopolymeric gel in contributing to strength development. Coexistence of C-S-H and geopolymer gels has been noted previously in various systems using $Ca(OH)_2$ or slag as calcium sources [9,13,14,17].

### 3.4. Characterisation by XRD

Fig. 1 shows the XRD diffractograms of the geopolymers with 20% GGBFS after 28 days using the three different activators (Matrices A1, A3 and A5), as well as the raw metakaolin and GGBFS used. The gypsum present in GGBFS was totally dissolved as a result of the alkaline activation. No significant new crystalline phase was detected, and the geopolymeric binders remained X-ray amorphous. All geopolymer diffractograms in this work display the characteristic 'geopolymer hump' at ~28–32° $2\theta$, attributable to aluminosilicate gel structures with or without nanoscale zeolitic character [3].

Fig. 2 shows the XRD diffractograms of the geopolymers with 20% cement at 28 days using $R=1.2$ (Matrix B5) and 2.0 (Matrix B1) as well as the raw metakaolin and cement used. The XRD pattern of the binder synthesised using $R=1.5$ (Matrix B3) is not shown, and is very similar to Matrices B1 and B5. Similar to the binders containing GGBFS (Fig. 1), there is no new crystalline peak detected in any binder. This is generally consistent with the results of Palomo et al. [32] for silicate activation of 30% fly ash–70% OPC mixtures, where the only new crystalline product observed after 28 days was $CaCO_3$ resulting from carbonation of the binder.

The diffractogram of the raw cement used (diffractogram CEM, Fig. 2) shows that cement contains several distinct peaks associated with crystalline calcium silicates and aluminates. Since there is no significant crystalline phase detected after alkaline activation except for a small amount of residual tricalcium silicate, it appears that the crystalline phases initially present have reacted. However, cement is specifically synthesised

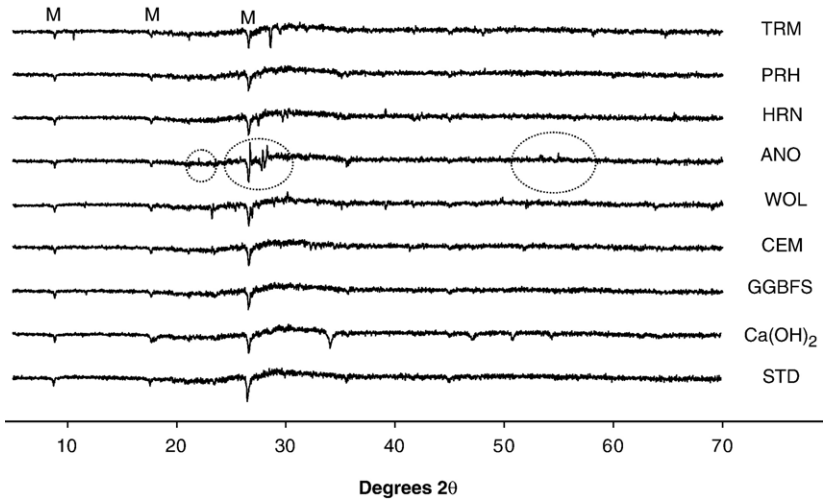


Fig. 4. Differences between the X-ray diffractograms before and after alkali activation ($R=1.2$) of metakaolin geopolymers with $Ca(OH)_2$ or calcium silicate minerals added at 20 mass %. M: changes due to muscovite dissolution. Circled peaks are specifically discussed in the text, and all 'dips' not marked correspond to the dissolution of the specific calcium silicates used in each sample.

to contain these specific crystalline phases due to their tendency to react and form hydrated products. So, this should not be taken *a priori* as an indication that all crystalline calcium silicates will likewise be reactive in geopolymerisation. The cement used here does also contain a significant quantity of tricalcium aluminate ($C_3A$), which is also expected to participate to some extent in the geopolymerisation reactions, although quite differently to the calcium silicate materials that are of primary interest here. Results showing the specific effects of calcium aluminate addition to geopolymers have not yet been published in detail.

Fig. 3 shows the XRD diffractogram of a geopolymer with 20% wollastonite and $R=1.2$ (Matrix C5), as well as the diffractograms of the raw materials used. The diffractograms of the geopolymers with $R=1.5$ and 2.0 are not shown, but were very similar to the diffractogram of Matrix C5. Unlike the systems with either cement or GGBFS, there are still significant amounts of undissolved wollastonite present after the alkaline activation for all alkaline conditions used, and this is a common feature found in all matrices synthesised from natural minerals (diffractograms not shown). This correlates well with the leaching data and the low strengths of these matrices, and supports the contention that this effect is at least in part due to gel network structure disruption effects.

To further analyse the effects of different calcium silicate sources on geopolymerisation, XRD difference plots were calculated between the binder at 28 days and the raw materials before activation (Fig. 4). $R=1.2$ was used in all samples shown, as the results for $R=1.5$ and 2.0 were very similar. The diffractogram labelled STD is a similar plot for a control sample with no calcium silicate, and a sample with 20 wt.% $Ca(OH)_2$ was also investigated for the sake of comparison. Fig. 4 shows that all difference patterns have similar characteristics. There is a sharp decrease in intensity at about 26.6–26.8° $2\theta$, corresponding to the dissolution of the muscovite impurity in the metakaolin and also shown by peaks at lower $2\theta$ angles in all samples. This is then followed by a gradual increase in intensity

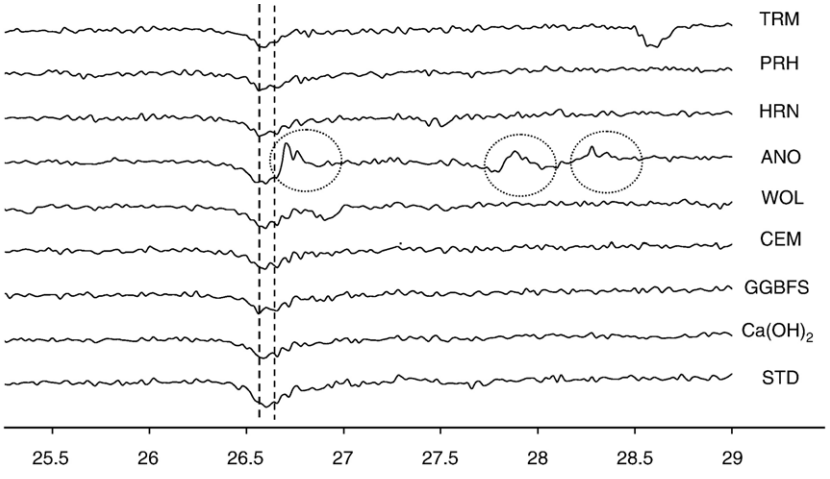


Fig. 5. Expanded view of the region of Fig. 4 between 25 and 29° $2\theta$. Dashed lines indicate the region 26.6–26.7° $2\theta$. Circled peaks are specifically discussed in the text.

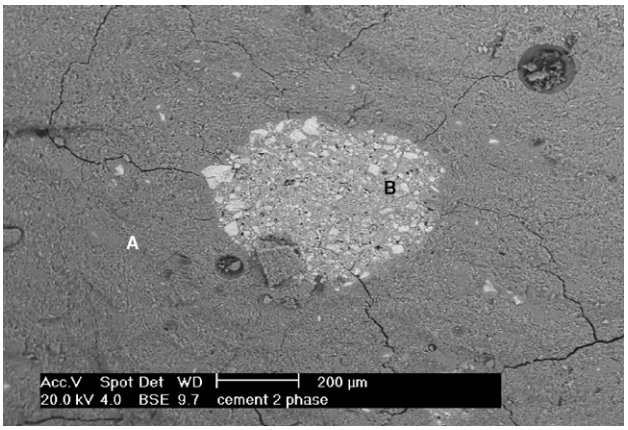


Fig. 6. SEM micrograph of Matrix B1 (20% cement, $R=2.0$) at 28 days. A: low-Ca geopolymeric binder, B: calcium silicate hydrate with a small proportion of aluminium.

until a maximum at around 29.5° 2$\theta$ matching the usual geopolymer peak position, then another decrease until 35° 2$\theta$. Fig. 5 highlights the difference patterns of Fig. 4 in the region between 25 and 29° 2$\theta$, showing that this trend is consistent across all samples studied. The weak peaks in the anorthite-containing specimen, observed at ~26.8 and 26.9° 2$\theta$ in Fig. 5, are tentatively attributed to the conversion of some of the muscovite-3T to the more stable, less ordered [33] muscovite-2M1 structure (PDF #6-0263). It is not clear why this should happen significantly in the anorthite-containing sample but not in any of the others. The peak just below 28° 2$\theta$ in this diffractogram (Fig. 5) further supports this suggestion, with a relatively strong peak in this region present in muscovite-2M1 but not in muscovite-3T, as do the small peaks between 22–24° and 52–56° 2$\theta$ in Fig. 4.

The small, relatively sharp reductions at specific 2$\theta$ angles in each diffractogram elsewhere in Figs. 4 and 5 are associated with the reaction of some of the crystalline phases present in the calcium silicate materials. All calcium silicates dissolved to some extent, however the extent of reaction depends on the mineralogy and thermal history of the calcium sources. The difference pattern of the sample with $Ca(OH)_2$ is similar to those with calcium silicates as Ca sources, indicating that the trends with regard to calcium release are largely independent of silica or alumina release from the minerals. Analysis of the microstructures of geopolymers with calcium silicate inclusions, and comparison of these results with previous work on the effects of $Ca(OH)_2$, will enable further analysis of this issue.

### 3.5. Microstructural analysis

Fig. 6 illustrates the microstructure of a geopolymeric product with 20% cement and $R=2.0$. Matrix B5, with $R=1.2$, displays a very similar phase-separated microstructure (not pictured). This appears relatively similar to the microstructure of the binder with 20% GGBFS (Matrix A1) as studied previously [9], with two separate phases coexisting. These are identified as geopolymeric and calcium silicate hydrate (C-S-H) gels respectively by X-ray microanalysis. The average concentration of calcium in the geopolymeric gel is less than 2 mol %. The semi-crystalline to crystalline C-S-H phases commonly formed as a result of the hydration of Portland cement are not formed in this alkaline activated system.

In contrast to the large amount of calcium precipitates found scattered in the MK–GGBFS binder synthesised using a highly alkaline system ($R=1.2$) as shown previously [9], the coexistence of both geopolymeric and C-S-H gels remains as the dominant feature found in the comparable MK–cement binder (Matrix B5). The growth of C-S-H within a geopolymeric gel upon the addition of cement is found to be independent of the alkalinity used within the range studied ($R=1.2$–$2.0$). This is likely to be the result of the higher availability of calcium and (particularly) silica from cement compared to GGBFS (Tables 3 and 4). The rapid release of silica as orthosilicic acid reduces the alkalinity of the activating solution, meaning that precipitation of $Ca(OH)_2$ is less favoured and leading to a greater extent of C-S-H formation. Thus, the coexistence of both gels remains the dominant microstructural feature of the alkaline activated MK–cement system (Fig. 6). This also provides an explanation for the greatly reduced effect of NaOH concentration in cement-containing systems compared to any others studied: The rapid release of $SiO_2$ from cement plays a buffering role, reducing the differences in alkalinity between the three activating solutions.

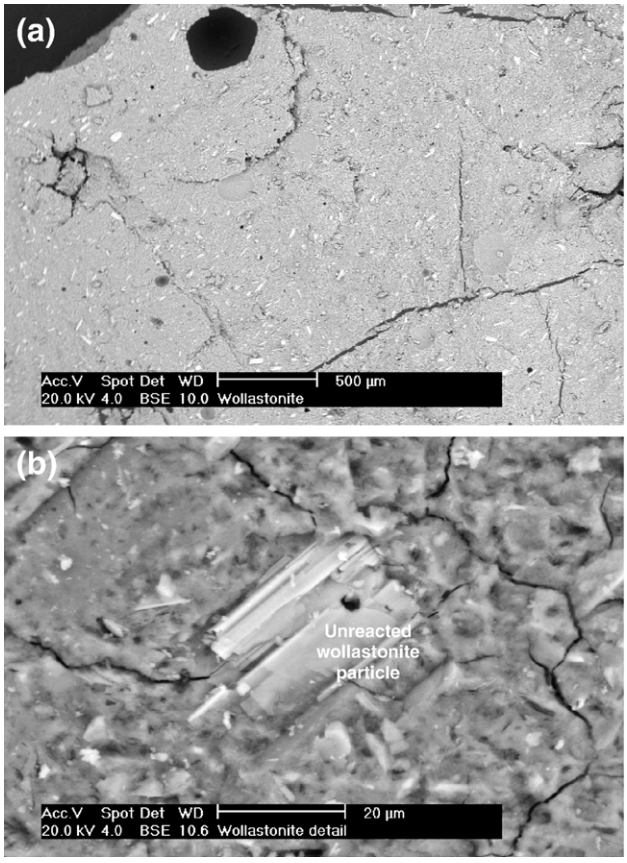


Fig. 7. SEM micrographs of Matrix C5 (20% wollastonite, $R=1.2$) at 28 days. Micrograph (b) shows a magnified view of (a), with a low-Ca geopolymeric binder surrounding the wollastonite particle.

Moreover, given that the size of the C-S-H gel regions formed in the geopolymeric gel is relatively large (~60–100 μm in diameter), the binding performance of the MK–cement system will not be based on the geopolymeric gel alone. Rather, similar to the MK–GGBFS binder synthesised at low alkalinity [9], the improved compressive strength achieved in the system is attributed to the coexistence of C-S-H and geopolymeric gels.

Fig. 7 shows the microstructure of the geopolymeric product with 20 wt.% of wollastonite added at $R=1.2$ (Matrix C5). These micrographs illustrate the most prominent feature found in systems containing crystalline calcium silicate minerals: unreacted mineral particles scattered in a low-Ca geopolymeric gel. The micrographs of matrices synthesised at $R=1.5$ and 2.0 are not shown, however they were found to have similar features. These SEM results are in agreement with the XRD data presented earlier. The reactivity of crystalline calcium silicate minerals is much lower than that of processed (less crystalline) calcium silicate sources (i.e. GGBFS or cement) in the alkaline activated system.

A clear coexistence between the geopolymeric and C-S-H phases could not be found in any of the systems containing natural calcium silicate minerals. Increasing the amount of crystalline calcium silicate added resulted only in binders with more unreacted particles situated within the geopolymeric gel. This corresponds to the strength decrease upon moving from 20% to 40% calcium silicate mineral addition observed in Section 3.3, as the loosely bound mineral particles interrupt the geopolymeric gel network structure. Elemental analysis of the geopolymeric gel formed in these systems showed that the average concentration of calcium is less than 1 mol%. The failure to form C-S-H – or in fact any other distinct Ca-containing phase – within the geopolymeric gel is likely to be the result of the lack of dissolved calcium species present in these systems.

## 4. Conclusion

The effects of different calcium silicate sources on geopolymerisation are highly dependent on the crystallinity and thermal history of the calcium silicate sources, as well as the alkalinity of the alkaline activator. Calcium dissolution from manufactured calcium silicate sources (blast furnace slag or Portland cement) at low alkalinity forms C-S-H gel in conjunction with the geopolymeric gel, enhancing strength. Less calcium dissolves from the natural calcium silicate minerals, so there is very little formation of C-S-H gel. The unreacted mineral particles then disrupt the geopolymeric gel network, resulting in lower overall strengths. This result also suggests that the coexistence of both geopolymeric gel and C-S-H gel gives rise to the satisfactory mechanical properties of the matrices synthesised at low alkalinities.

Geopolymeric gel appears to be the dominant product formed at high alkalinities. Calcium plays a lesser role in affecting the nature of the end product, thus the extent of dissolution of calcium species from the different calcium silicate sources will not have a major impact on the resultant strength of the matrices. Subsequently, the compressive strengths of the matrices synthesised at high alkalinity were found to be similar regardless of the types of calcium silicate minerals used.

## Acknowledgements

The financial support received from the Australian Research Council (ARC), the Particulate Fluids Processing Centre (a Special Research Centre of the ARC), and the US Air Force Office of Scientific Research/Asian Office of Aerospace Research and Development (AOARD), under Contract AOARD 02-33, is greatly appreciated.

## References

[1] J. Davidovits, Geopolymers — inorganic polymeric new materials, J. Therm. Anal. 37 (8) (1991) 1633–1656.
[2] A. Palomo, M.W. Grutzeck, M.T. Blanco, Alkali-activated fly ashes — a cement for the future, Cem. Concr. Res. 29 (8) (1999) 1323–1329.
[3] J.L. Provis, G.C. Lukey, J.S.J. van Deventer, Do geopolymers actually contain nanocrystalline zeolites? — A reexamination of existing results, Chem. Mater. 17 (12) (2005) 3075–3085.
[4] P. Duxson, A. Fernández-Jiménez, J.L. Provis, G.C. Lukey, A. Palomo, J.S.J. van Deventer, Geopolymer technology: the current state of the art, J. Mater. Sci. 42 (9) (2007) 2917–2933.
[5] J.S.J. van Deventer, J.L. Provis, P. Duxson, G.C. Lukey, Reaction mechanisms in the geopolymeric conversion of inorganic waste to useful products, J. Hazard. Mater. A139 (3) (2007) 506–513.
[6] P.V. Krivenko, Alkaline cements, in: P.V. Krivenko (Ed.), Proceedings of the First International Conference on Alkaline Cements and Concretes, VIPOL Stock Company, Kiev, Ukraine, 1994, pp. 11–129.
[7] J.G.S. van Jaarsveld, J.S.J. van Deventer, A. Schwartzman, The potential use of geopolymeric materials to immobilise toxic metals: part II. Material and leaching characteristics, Miner. Eng. 12 (1) (1999) 75–91.
[8] M.L. Granizo, S. Alonso, M.T. Blanco-Varela, A. Palomo, Alkaline activation of metakaolin: effect of calcium hydroxide in the products of reaction, J. Am. Ceram. Soc. 85 (1) (2002) 225–231.
[9] C.K. Yip, J.S.J. van Deventer, Microanalysis of calcium silicate hydrate gel formed within a geopolymeric binder, J. Mater. Sci. 38 (18) (2003) 3851–3860.
[10] K. Dombrowski, A. Buchwald, M. Weil, The influence of calcium content on the structure and thermal performance of fly ash based geopolymers, J. Mater. Sci. 42 (9) (2007) 3033–3043.
[11] A. Buchwald, H. Hilbig, C. Kaps, Alkali-activated metakaolin-slag blends — performance and structure in dependence on their composition, J. Mater. Sci. 42 (9) (2007) 3024–3032.
[12] A. Allahverdi, F. Škvára, Nitric acid attack on hardened paste of geopolymeric cements — part 1, Ceram.-Silik. 45 (3) (2001) 81–88.
[13] S. Alonso, A. Palomo, Calorimetric study of alkaline activation of calcium hydroxide–metakaolin solid mixtures, Cem. Concr. Res. 31 (1) (2001) 25–30.
[14] S. Alonso, A. Palomo, Alkaline activation of metakaolin and calcium hydroxide mixtures: influence of temperature, activator concentration and solids ratio, Mater. Lett. 47 (1–2) (2001) 55–62.
[15] A. Buchwald, C. Kaps, M. Hohmann, Alkali-activated binders and pozzolan cement binders — complete binder reaction or two sides of the same story? Proceedings of the 11th International Conference on the Chemistry of Cement, Portland Cement Association, Durban, South Africa, 2003, pp. 1238–1246.
[16] C.L. Nicholson, R.A. Fletcher, N. Miller, C. Stirling, J. Morris, S. Hodges, K.J.D. MacKenzie, M. Schmücker, Building innovation through geopolymer technology, Chem. N. Z. (Sept 2005) 10–12.
[17] C.K. Yip, G.C. Lukey, J.S.J. van Deventer, The coexistence of geopolymeric gel and calcium silicate hydrate at the early stage of alkaline activation, Cem. Concr. Res. 35 (9) (2005) 1688–1697.
[18] S.K. Lee, J.F. Stebbins, The degree of aluminum avoidance in aluminosilicate glasses, Am. Miner. 84 (5–6) (1999) 937–945.
[19] J.L. Provis, P. Duxson, G.C. Lukey, J.S.J. van Deventer, A statistical thermodynamic model for Si/Al ordering in amorphous aluminosilicates, Chem. Mater. 17 (11) (2005) 2976–2986.

[20] F.J. Silva, C. Thaumaturgo, Fibre reinforcement and fracture response in geopolymeric mortars, Fatigue Fract. Eng. Mater. Struct. 26 (2) (2003) 167–172.
[21] W.K.W. Lee, J.S.J. van Deventer, The interface between natural siliceous aggregates and geopolymers, Cem. Concr. Res. 34 (2) (2004) 195–206.
[22] W.K.W. Lee, J.S.J. van Deventer, Chemical interactions between siliceous aggregates and low-Ca alkali-activated cements, Cem. Concr. Res. 37 (6) (2007) 844–855.
[23] H. Xu, J.S.J. van Deventer, The geopolymerisation of alumino-silicate minerals, Int. J. Miner. Proc. 59 (3) (2000) 247–266.
[24] J.L. Provis, J.S.J. van Deventer, Geopolymerisation kinetics. 2. Reaction kinetic modelling, Chem. Eng. Sci. 62 (9) (2007) 2318–2329.
[25] E.H. Oelkers, J. Schott, J.L. Devidal, The effect of aluminum, pH, and chemical affinity on the rates of aluminosilicate dissolution reactions, Geochim. Cosmochim. Acta 58 (9) (1994) 2011–2024.
[26] S.L. Brantley, Y. Chen, Chemical weathering of pyroxenes and amphiboles, in: A.F. White, S.L. Brantley (Eds.), Chemical Weathering Rates of Silicate Minerals, Reviews in Mineralogy, vol. 31, Mineralogical Society of America, Washington DC, 1995, pp. 119–172.
[27] S.V. Golubev, O.S. Pokrovsky, J. Schott, Experimental determination of the effect of dissolved $CO_2$ on the dissolution kinetics of Mg and Ca silicates at 25 °C, Chem. Geol. 217 (3–4) (2005) 227–238.
[28] W.K.W. Lee, J.S.J. van Deventer, The effect of ionic contaminants on the early-age properties of alkali-activated fly ash-based cements, Cem. Concr. Res. 32 (4) (2002) 577–584.
[29] P. Duxson, J.L. Provis, G.C. Lukey, S.W. Mallicoat, W.M. Kriven, J.S.J. van Deventer, Understanding the relationship between geopolymer composition, microstructure and mechanical properties, Colloids Surf., A Physicochem. Eng. Asp. 269 (1–3) (2005) 47–58.
[30] P. Duxson, S.W. Mallicoat, G.C. Lukey, W.M. Kriven, J.S.J. van Deventer, The effect of alkali and Si/Al ratio on the development of mechanical properties of metakaolin-based geopolymers, Colloids Surf., A Physicochem. Eng. Asp. 292 (1) (2007) 8–20.
[31] J.W. Phair, J.S.J. van Deventer, J.D. Smith, Mechanism of polysialation in the incorporation of zirconia into fly ash-based geopolymers, Ind. Eng. Chem. Res. 39 (8) (2000) 2925–2934.
[32] A. Palomo, A. Fernández-Jiménez, G.Y. Kovalchuk, L.M. Ordoñez, M.C. Naranjo, OPC–fly ash cementitious systems. Study of gel binders formed during alkaline hydration, J. Mater. Sci. 42 (9) (2007) 2958–2966.
[33] N. Güven, C.W. Burnham, The crystal structure of 3T muscovite, Z. Kristallogr. 125 (1–6) (1967) 163–183.